

Estimating the Lunar Core Equatorial Ellipticity using Lunar Laser Ranging

Vishnu Viswanathan^{1,2}, Erwan Mazarico¹, Sander Goossens^{1,2}, Nicolas Rambaux³, David Smith⁴

¹ NASA Goddard Space Flight Center, Greenbelt, MD; ² CRESST II, University of Maryland, Baltimore County, MD; ³ IMCCE, Observatoire de Paris, Université Pierre et Marie Curie, Paris 75014, ⁴ EAPS, Massachusetts Institute of Technology, Cambridge, MA

Abstract ID: 2031

A. Introduction

Lunar Laser Ranging involves precise millimeter-level tracking of five retroreflectors on the near-side lunar surface.

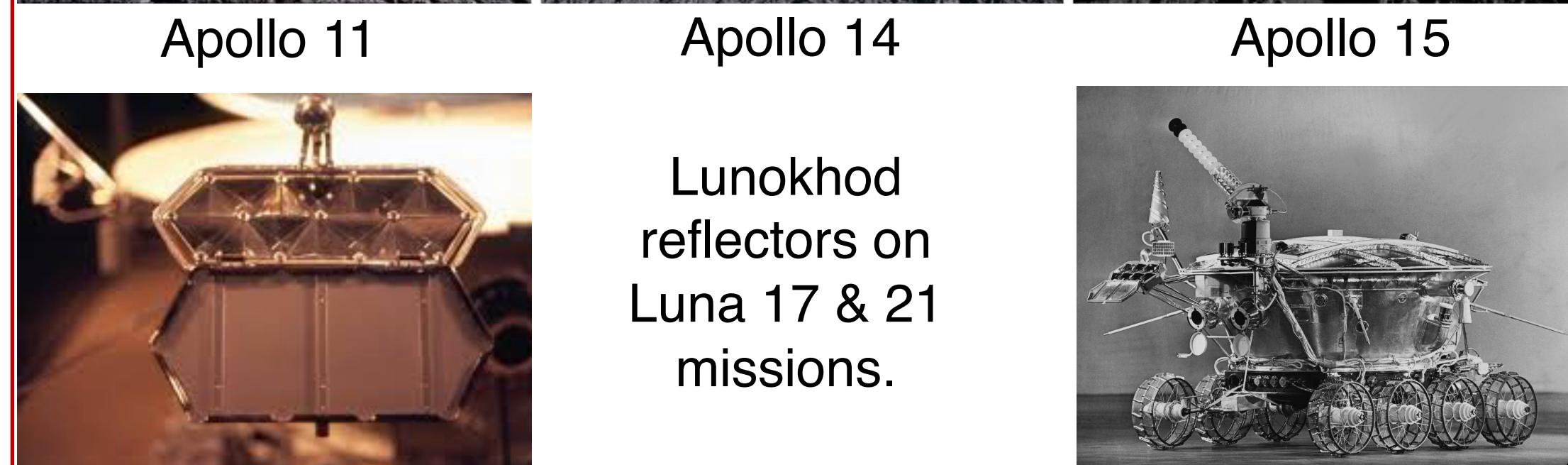
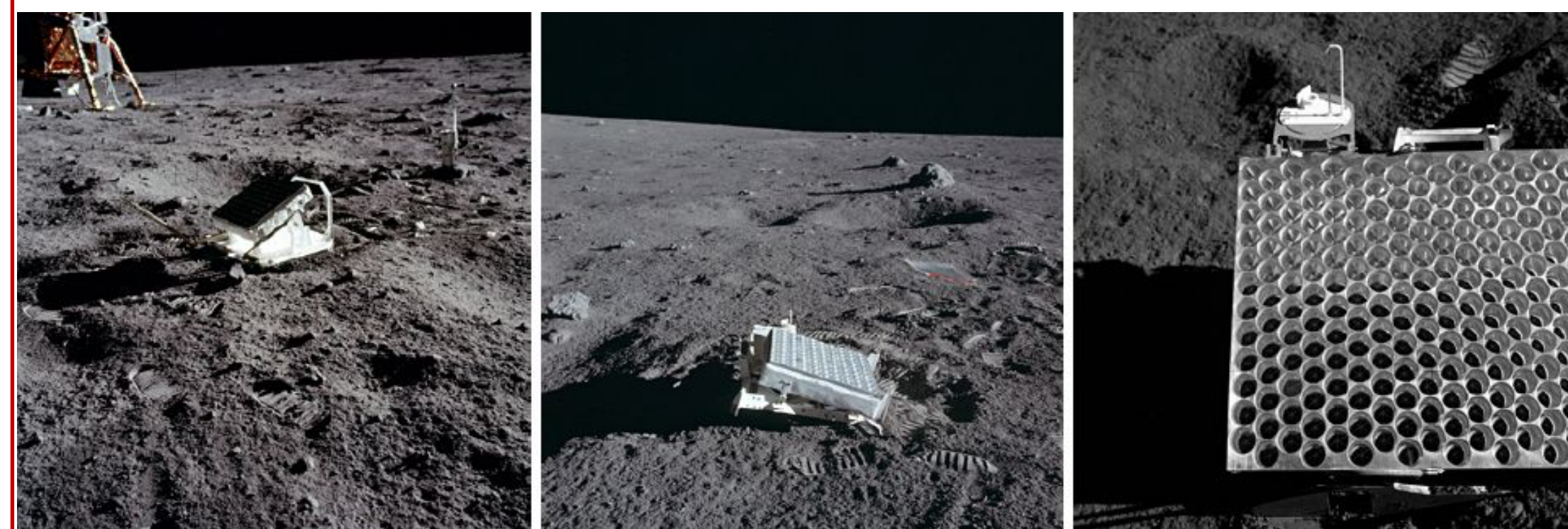


Fig. 1: Lunar retroreflector arrays



Fig. 2: Present and future LLR stations (ILRS)

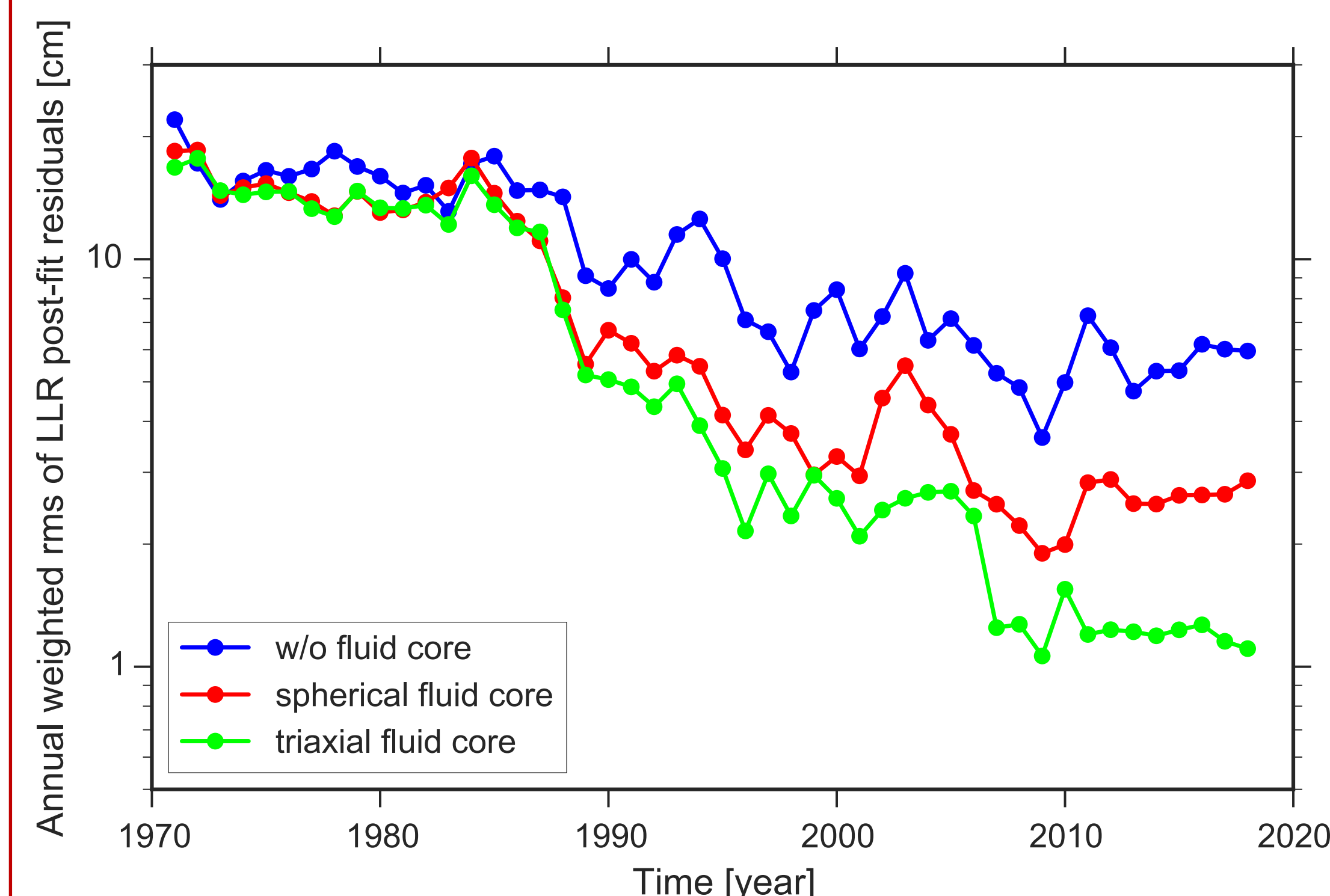


Fig. 3: LLR post-fit residuals (1-way light time).
Blue - Model without a fluid core;
Red - Model with a spherical fluid core;
Green - Model with a triaxial fluid core^[5].

B. Methodology

How does tracking surface reflectors help understand interior structure?

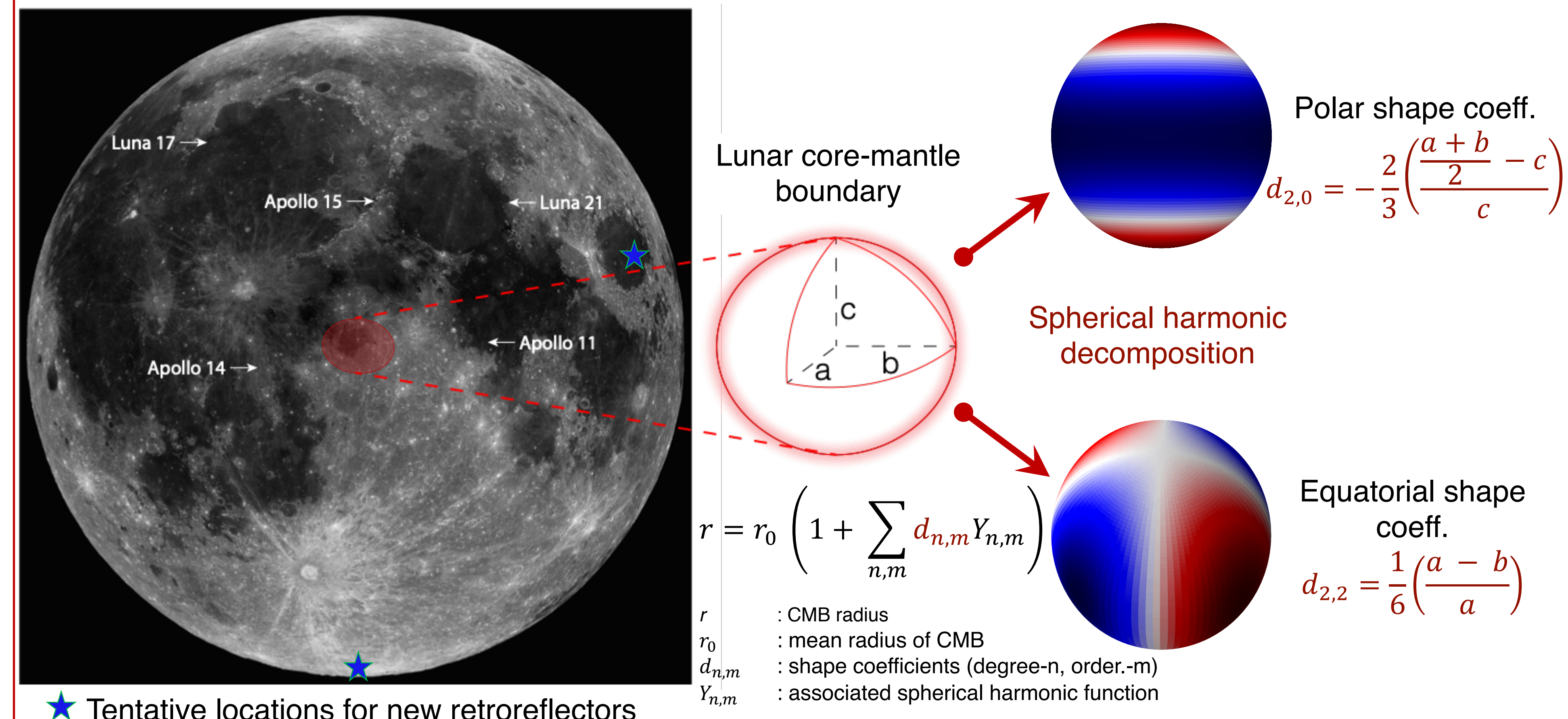
Monitoring the rotation of a body gives us clues to understanding its interior structure. i.e. a moon with a fluid core rotates differently from one with a solid core. Angular momentum is exchanged between the layers of the Moon as it rotates and orbits around the Earth.

Euler-Liouville equation for (a) the Moon and (b) the fluid core :

$$\frac{d}{dt}(I\Omega + I_c\omega_c) + \Omega \times (I\Omega + I_c\omega_c) = \Gamma^{\text{external}} \quad (a)$$

$$\frac{d}{dt}I_c(\Omega + \omega_c) + \Omega \times I_c(\Omega + \omega_c) = \Gamma_c^{\text{friction}} + \Gamma_c^{\text{inertial}} \quad (b)$$

I, I_c : Moment of inertia of the Moon, Moon's core
 Ω, ω_c : Angular velocity of the Moon, fluid core (relative)
 Γ^{external} : Torques (external) acting on the Moon
 Γ^{friction} : Torques from viscous friction at CMB
 Γ^{inertial} : Torques from flow along non-spherical boundary



★ Tentative locations for new retroreflectors

Q1: What do we currently know about the lunar core from the LLR data ?

- Viscous friction from relative motion at the core-mantle boundary (CMB) – spherical core model^[1]
- Polar oblateness for a given core moment – axisymmetric core model^[2,3,4]
- Polar oblateness and radius for a relaxed lunar core with plausible non-principal axis tilt – triaxial core model^[5]

Q2: Can we detect the CMB equatorial ellipticity from LLR data ?

- Yes, LLR is sensitive to this parameter. But, presently remains unresolved.
- Extended high-precision data will enable detection.
- The next generation of lunar retroreflectors flown by commercial lander(s) and the Artemis program will strengthen detection and reduce data span requirements by almost a decade! See Fig. 6.

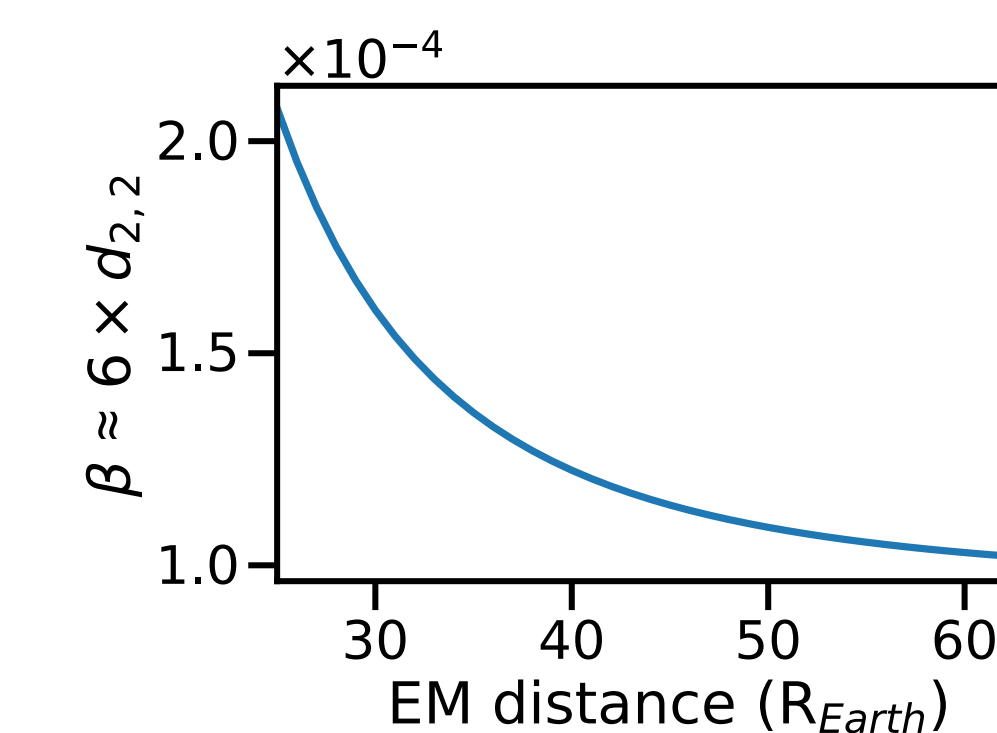


Fig. 4: Core ellipticity with EM distance^[6,9]

Q3: What can we learn from the CMB equatorial ellipticity ?

- **Lunar evolution:** At first order, CMB equatorial ellipticity and Ekman number would help determine the threshold for the development of elliptical instabilities in the lunar core. The former particularly influences the growth rate of such instabilities – a mechanism to power lunar dynamos in the past^[6].
- **Lunar rotational dynamics and interior structure:** The CMB equatorial ellipticity will modify the lunar free core nutation (FCN) and induce a new proper mode (analogous to the Chandler Wobble). It would also help confirm the current relaxed state of the lunar core^[5].

C. Simulations

- LLR covariance matrix with 150 parameters.
- Fractional uncertainty from calibrated error-covariance (VCE)^[7]
- Simulated data from Grasse (G), Apache Point (A) and HartRAO (S) with 1 hour per day (~10 min per normal point) with a precision of ~7 mm in 1-way range.
- Two new retroreflectors – near Crisium crater (upcoming CLPS lander) and South Pole (Artemis lander).
- Degree-2 order-2 shape of the lunar CMB is assumed to be 5 times larger than a relaxed core within a non-hydrostatic lithosphere^[5,6].

Fig. 5: Sensitivity of lunar rotation to lunar core equatorial ellipticity.

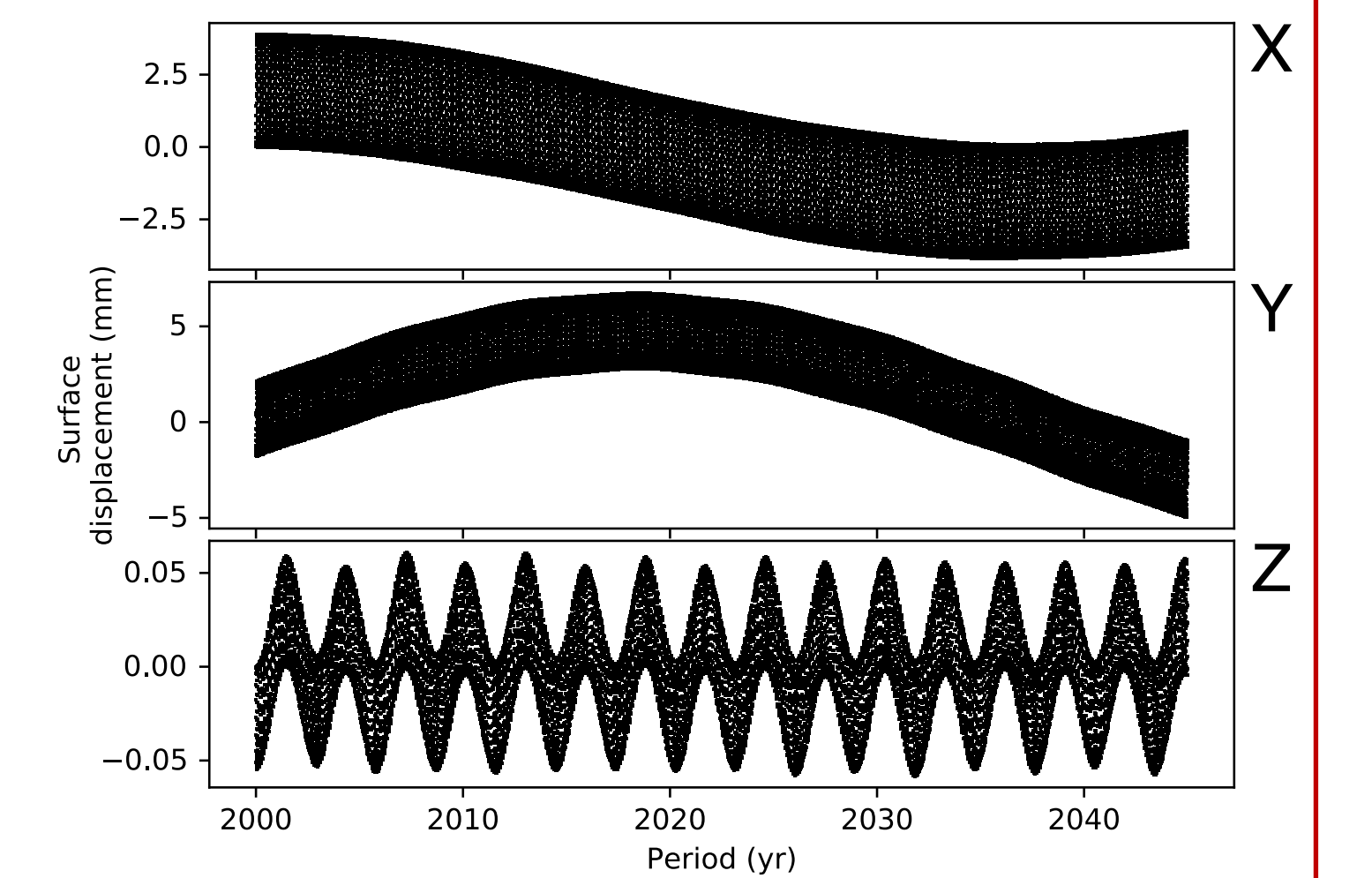
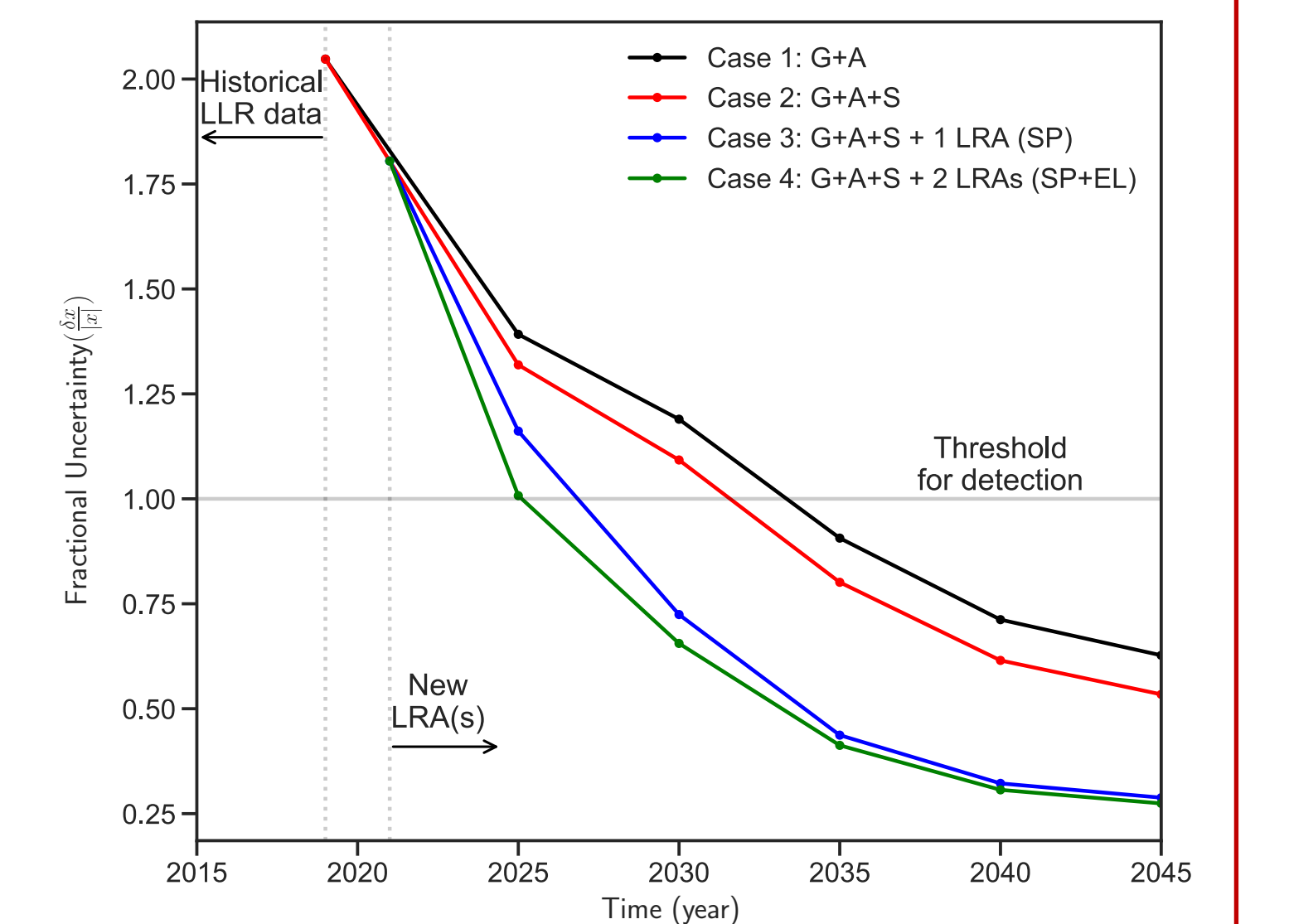


Fig. 6: Recovering the lunar core equatorial ellipticity



References

- [1] Williams *et al.* *JGR:Pla.* **106**, 27933–27968 (2001). [2] Folkner *et al.* *IPNR.* **42-196** (2014). [3] Pavlov, *et al.* *CMDA.* **126**, 61–88 (2016). [4] Viswanathan, *et al.* *MNRAS.* **476**, 1877–1888 (2018). [5] Viswanathan, *et al.* *GRL.* **46**, 7295–7303 (2019). [6] Le Bars, *et al.* *Nat.* **479**, 215–218 (2011). [7] Lemoine *et al.* *JGR:Pla.* **118**, 1676–1698 (2013). [8] Fienga *et al.* *NSTIM.* **109** (2019). [9] Wieczorek, *et al.* *JGR:Pla.* **124**, 1410–1432 (2019). [10] Wieczorek & Meschede, *GSG.* **19**, 2574–2592 (2018).

Acknowledgment

Support for this research was provided by NASA's Planetary Science Division Research Program through the CRESST II cooperative agreement. The LLR (real and simulated) data were processed using a triaxial core model developed in the INPOP planetary and lunar ephemeris^[8] and GINS software. The hydrostatic core shape was computed using SHTools^[10]. Authors acknowledge LLR observers and their five decades of accurate measurements, archived at <http://polac.obspm.fr>